Semiconductor Physics, Quantum Electronics & Optoelectronics, 2016. V. 19, N 4. P. 321-327.
doi: https://doi.org/10.15407/spqeo19.04.321

PACS 81.07.Ta, 68.65.Hb, 68.37.Xy

Drift correction of the analyzed area during the study of the lateral elemental composition distribution in single semiconductor nanostructures by scanning Auger microscopy

S.S. Ponomaryov*, V.O. Yukhymchuk, M.Ya. Valakh
V. Lashkaryov Institute of Semiconductor Physics, National Academy of Sciences of Ukraine,
41, prospect Nauky, 03028 Kyiv, Ukraine
**Correspondence e-mail: s.s.ponomaryov@gmail.com; phone: +38(095)-457-02-28*

Abstract. The main difficulty in obtaining the lateral elemental composition distribution maps of the semiconductor nanostructures by Scanning Auger Microscopy is the thermal drift of the analyzed area, arising from its local heating with the electron probe and subsequent shift. Therefore, the main goal of the study was the development of the effective thermal drift correction procedure. The measurements were carried out on GeSi/Si nanoislands obtained with molecular beam epitaxy by means of Ge deposition on Si(100) substrate. Use of the thermal drift correction procedure made it possible to get the lateral elemental composition distribution maps of Si and Ge for various types of GeSi/Si nanoislands. The presence of the germanium core and silicon shell in both the dome GeSi/Si nanoislands and pyramid ones was established. In the authors' opinion, this type of elemental distribution is a result of the completeness of the interdiffusion processes course in the island/wetting layer/substrate system, which play the key role in the nucleation, evolution and growth of GeSi/Si nanoislands. The proposed procedure of the thermal drift correction of the analyzed area allows direct determination of the lateral composition distribution of the GeSi/Si nanoislands with the size of the structural elements down to 10 nm.

Keywords: thermal drift correction, GeSi/Si nanoislands, lateral composition distribution.

Manuscript received 01.06.16; revised version received 14.09.16; accepted for publication 16.11.16; published online 05.12.16.

1. Introduction

In recent decades, nanoobjects with charge carriers subjected to three-dimensional confinement attract considerable interest of researchers. Spatial confinement of charge carriers leads to the splitting of the system energy levels, providing atomic properties of such objects (quantum dots or nanoislands). Shape, size, elemental composition and elastic stress field distribution in nanoislands' bulk define their energy spectrum.

Control of both individual and group quantum dots characteristics opens new horizons of possibilities for their practical applications in lasers, communication systems, quantum informatics (computations) and photonics [1-4]. Also, it should be noted that GeSi/Si nanoislands are easily compatible with already existing and widespread silicon technology, which allows easy integration of quantum dots in micro- and optoelectronic components.

Understanding the nucleation and evolution nature of the quantum dots is of fundamental importance from the viewpoint of quantum mechanics and materials science.

It is important to control the values of the discrete energy levels of individual GeSi/Si nanostructures for the successful practical application of quantum dots in

different industrial sectors. It is known that the elastic stress distribution in the defect-free nanoislands depends exceptionally on chemical composition distribution. Therefore, the detailed study of this characteristic is a first-priority for understanding the atomic properties of investigated nanostructures.

The significant amount of methods for the study of structural parameters and nanostructures chemical composition, including a combination of microscopic, spectroscopic, diffraction methods, and sometimes chemical etching is used nowadays [5]. Despite the great variety of methods, each of them has a number of advantages and drawbacks, as a result, the data obtained by these methods has a contradictory character [6-8].

Raman spectroscopy [9-11], X-ray diffraction [12], X-ray photoelectron spectroscopy and Auger electron spectroscopy (AES) are widely used for characterization of the nanoislands, however, they have a low locality and provide averaged information over a statistical ensemble of the nanostructures. Transmission electron microscopy (TEM) in combination with electron energy loss spectroscopy (EELS) or energy-dispersive X-ray spectroscopy (EDX) provides high spatial resolution [13]. However, EELS and EDX require a long period of spectra registration. On the other hand, the sample preparation process for TEM measurements is protracted and complicated. The surface sample area suitable for analysis is sufficiently small for reliable statistical results and data obtained in the process of the chemical composition analysis by TEM are averaged along the vertical axis (axis of the probe). Another drawback of the technique is the uncertainty of the foil surface area position for analysis relatively to the nanoislands growth axis. All of the above-mentioned drawbacks in the sample preparation procedure are also inherent to scanning tunneling microscopy, which determines the crystal lattice distortion at the atomic level. At the same time, determination of the elemental composition using the elastic stress fields distribution in the cluster's bulk is not trivial. Another interesting technique is a combination of atomic force microscopy and selective chemical etching [14-17]. Alternate etching procedure and sample scanning give the representation of the surfaces with the identical chemical composition. However, the presence of the strong elastic stress fields distorts the quantum dot surface geometry, on the one hand, and affects the selective etching rate, on the other hand.

2. Materials and methods

Use of scanning Auger microscopy (SAM) for studying the individual nanoislands composition is promising due to high locality of the technique [18]. The lateral size of analyzed area can reach down to 3…5 nm, and Auger-electron escape depth is about 1 nm [19]. The pioneering works in application of SAM to study the elemental composition of individual GeSi/Si nanoislands were performed by Maximov et al. [20]. However, the low spatial resolution of the used instrument has allowed working only with objects having the lateral sizes from 125 up to 600 nm, which is much higher than that of nanostructures sizes being of practical interest. It's inevitable to have a deal with the problem of analyzed area drift during long-time registration of the Auger spectra and at reducing the size of investigation objects. Effective compensation of this shift is a key problem when registering the lateral elemental composition distribution on the sample surface containing GeSi/Si nanoislands.

Objects of investigation in this study are arrays of GeSi nanoislands formed under the self-induced Stranski–Krastanov growth mode using "BALZERS" molecular beam unit under the residual atmospheric pressure of 10^{-7} – 10^{-8} Pa [21].

The study was performed using two samples. A1 sample was obtained by Ge deposition on Si (100) substrate at the temperature 700 °C and deposition rate 0.07 Å/s. The nominal thickness of the Ge layer was 8.7 monolayers (ML). The buffer layer containing 10 at.% of Ge with the 10-nm thickness was grown on the Si (100) substrate on A2 specimen before Ge deposition. Germanium film with the nominal thickness of 8 ML was deposited on the buffer layer with the same rate and at the same temperature as in the case of A1 specimen.

The investigation was performed on the scanning Auger microprobe JAMP-9500F of JEOL production (Japan) with the spatial resolution in the secondary electron image mode of 3 nm. The instrument is equipped with the hemispherical Auger electrons analyzer with the energy resolution $\Delta E/E$ of 0.05 to 0.6% and the ion gun for the layer-by-layer analysis with Ar^+ ion accelerating voltage of 10 to 4000 V. The diameter of ion beam is about 120 μm, and the vacuum of the specimen chamber was better than $5 \cdot 10^{-7}$ Pa.

3. Results

The main goal of the study is to obtain high spatial resolution maps of the elemental composition distribution on the GeSi/Si nanoislands and wetting layer surface [22]. Based on the above-mentioned maps, it is possible to determine the character of Ge and Si distribution in the cluster bulk and evaluate the scale and role of the interdiffusion in the process of nucleation, evolution, and growth of GeSi/Si nanostructures.

The nanoislands' lateral sizes of practical interest lie within the range from 5 to 100 nm. The study of such objects requires the use of high spatial resolution operation modes.

It is necessary to use the minimal diameter of the electron probe in the above-mentioned modes, which can be only achieved by reducing its current. On the other hand, decreasing the probe current leads to disastrous declining of the Auger signal intensity, and it is vital significantly to increase the signal registration time (from 3 to 15 hours) to obtain the acceptable signal-to-noise ratio during Auger spectra and maps registration.

Semiconductor Physics, Quantum Electronics & Optoelectronics, 2016. V. 19, N 4. P. 321-327.
doi: https://doi.org/10.15407/spqeo19.04.321

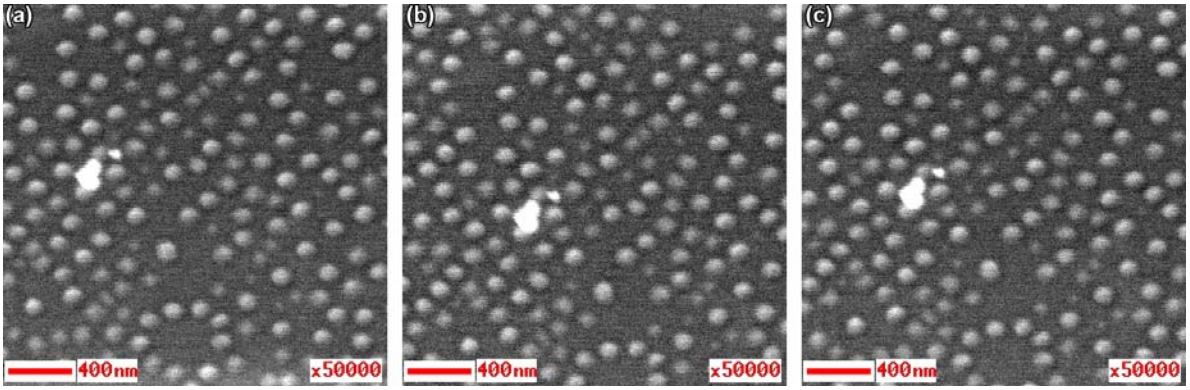

Fig. 1. The series of three successive secondary electron images of the analyzed sample area registered with an interval of 90 s.

The drift of the analyzed area during the measurement process

The drift of the analyzed area during the measurement process is the critical problem in operation modes with high locality. The sequence of the GeSi/Si nanoislands pictures in the secondary electron mode recorded for the intervals of 90 s is shown in Fig. 1. As seen from this figure, the investigated section of the sample surface moves smoothly, chaotically wandering around the initial position. According to our observations, the diameter of such wandering region can be up to 100 nm and displacement velocity of the analyzed object – up to 20 nm/s. It follows from the aforesaid that the measurement time for which the investigated object haven't enough time to shift by a significant distance (*e.g.*, 0.1 of the analyzed object diameter) should not exceed 25…30 s. It is obvious that the stated time is insufficient for significant Auger signal accumulation at the low probe current required to obtain the high-resolution image. Thus, the Auger signal registration of such objects is possible only in the case of its accumulation in the series of a large number of short successive measurements in combination with correction of the analyzed object position each time after every this measurement.

The proposed correction procedure removes aftereffects of the analyzed area drift and does not eliminate its reasons. So, the issue of clarifying the nature of the effect is not essential for us. Nevertheless, let's say a few words regarding this issue. It is widely believed that the drift of the analyzed area under the electron probe is caused by electric charge [20]. In other words, it is believed that accumulation of the negative charge on the sample surface due to its low electrical conductivity creates an electric field that can shift the high-energy electrons of the primary beam (30 keV) from their initial trajectory. According to our observations, the charging effect begins to appear first on the low-energy electrons. In the case of charging, the Auger peaks were primarily shifted from their standard energy positions and then the whole Auger spectrum was deformed starting with the low-energy range. Further intensification of charging leads to a change in the brightness of the secondary electron image: brightness spontaneously and gradually rises to a certain level and then comes to its dramatic disruption. Numerous bands of the abrupt image shift appear on the secondary electron image under strong charging that are accompanied by spontaneous modulation of the brightness. The above-mentioned attributes of charging are not observed in our case. Moreover, the ability of the charging neutralization of the dielectric samples by irradiation of them with the low-energy Ar^+ ion beam is provided in the Auger microprobe JAMP 9500F. The use of the specified procedure to the Ge/Si samples did not influence the observed character of the analyzed area drift. All these facts do not testify in favor of the electrical nature of the drift. We tend to consider that the analyzed area drift has a thermal nature. Local heating the analyzed sample site with following thermal expansion occurs due to the low thermal conductivity of the sample under the electron probe, which leads to the smooth drift of the analyzed area. It should be added for completeness of this issue that the drift effect is practically absent (hardly observed) on the copper samples with high electrical and thermal conductivity characteristics.

The procedure of the thermal drift correction

The principle of the successive comparison at regular time intervals of the analyzed area initial image and the current one subjected to the drift with its subsequent compensation was the basis for the developed procedure of thermal drift correction. This correction was performed every 10–15 s. A single raster line of the Auger map was recorded for this time, and the array of GeSi/Si nanoislands exactly does not shift to a distance more than 10 nm. The positioning accuracy during matching these two images was ±3.5 nm. The ultimate spatial resolution of the registered Auger maps was practically defined by the above-mentioned parameters.

Let us illustrate the effect of thermal drift procedure application. The Auger maps of germanium (a) and silicon (b) registered on the same surface section of A1 sample containing GeSi/Si nanostructures at magnification ×50 000 without thermal drift correction are shown in Fig. 2. The analytical Auger peaks of Ge_{LMM} with the energy 1147 eV and Si_{LVV} with the energy 92 eV were used for registration of the specified maps. Each map consisted of 256 lines, and each line contains 256 pixels. The single line of the germanium Auger map was recorded for the total time of 100 s due to the low intensity of the Ge_{LMM} peak, while the single line registration time of intensive Si_{LVV} peak was only 20 s. Thus, the total acquisition time for the obtained Auger maps for Ge and Si was ~7 and 1.5 hours, respectively. In Fig. 2, as further for all Auger maps, hot color corresponds to a high content of the analyzed element, while a cold color – to its low content.

Ge (a) and Si (b) Auger maps of the same surface section of A1 sample, as in Fig. 2, registered using thermal drift correction are shown in Fig. 3. The single line registration time of Ge Auger map was 10 s, which prevented the shift of the GeSi/Si nanoislands array to the significant distance. Immediately thereafter, the above-described procedure of image drift correction was performed for 11 s. The specified line registration time was not enough for accumulation of acceptable signal-to-noise ratio of the Auger map. Therefore, 9 additional passes through the same raster with subsequent summation were performed to improve this ratio during map registration. Thus, the total acquisition time of the single line signal reached the same 100 s as in the case of Fig. 2a. As a result, the total registration time of the Ge Auger map, including signal acquisition time and image drift correction, was ~15 hours. The same operation mode was used for Si Auger map registration (Fig. 3b). Image drift correction was performed after each line registration, which lasted 10 s. In this case, two passes through the raster were enough to achieve the acceptable signal-to-noise ratio. As a result, the total analysis time of the single line was 20 s, as in the case of Fig. 2b, and the total registration time of the Si Auger map was ~3 hours. Comparison of the Auger maps quality shown in Figs. 2 and 3 leads to a conclusion about the efficiency of using the proposed image drift correction procedure for the elemental composition distribution investigation of structures with nanometric sizes.

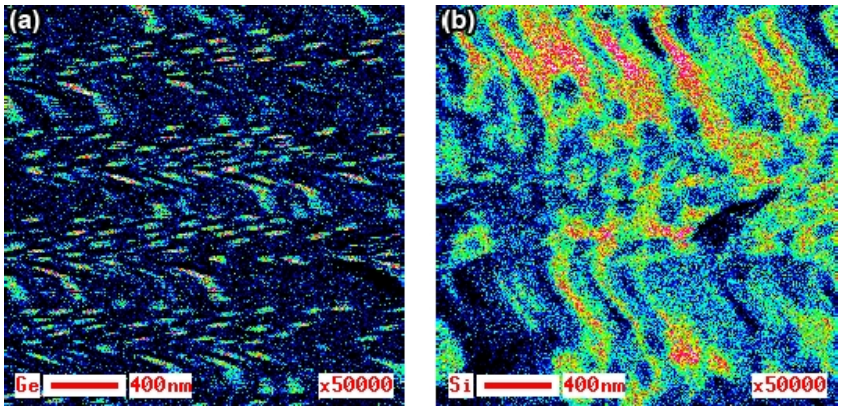

Fig. 2. Ge (a) and Si (b) Auger maps of the analyzed surface section of A1 sample under magnification 50 000 without thermal drift correction.

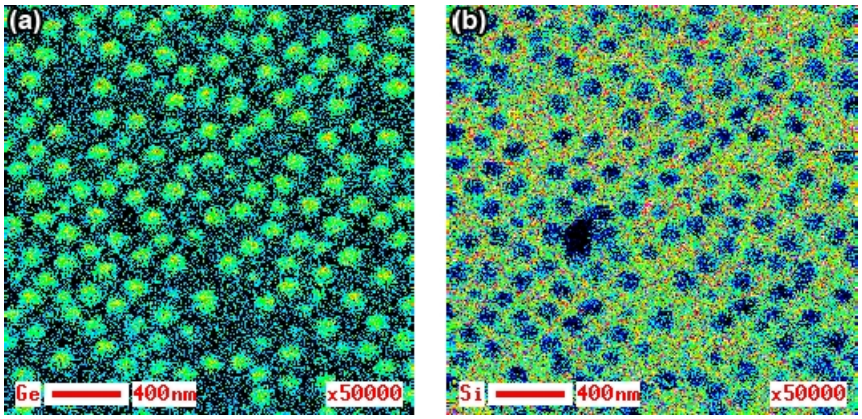

Fig. 3. Ge (a) and Si (b) Auger maps of the same analyzed surface section of A1 sample under magnification 50 000 with thermal drift correction.

Semiconductor Physics, Quantum Electronics & Optoelectronics, 2016. V. 19, N 4. P. 321-327.
doi: https://doi.org/10.15407/spqeo19.04.321

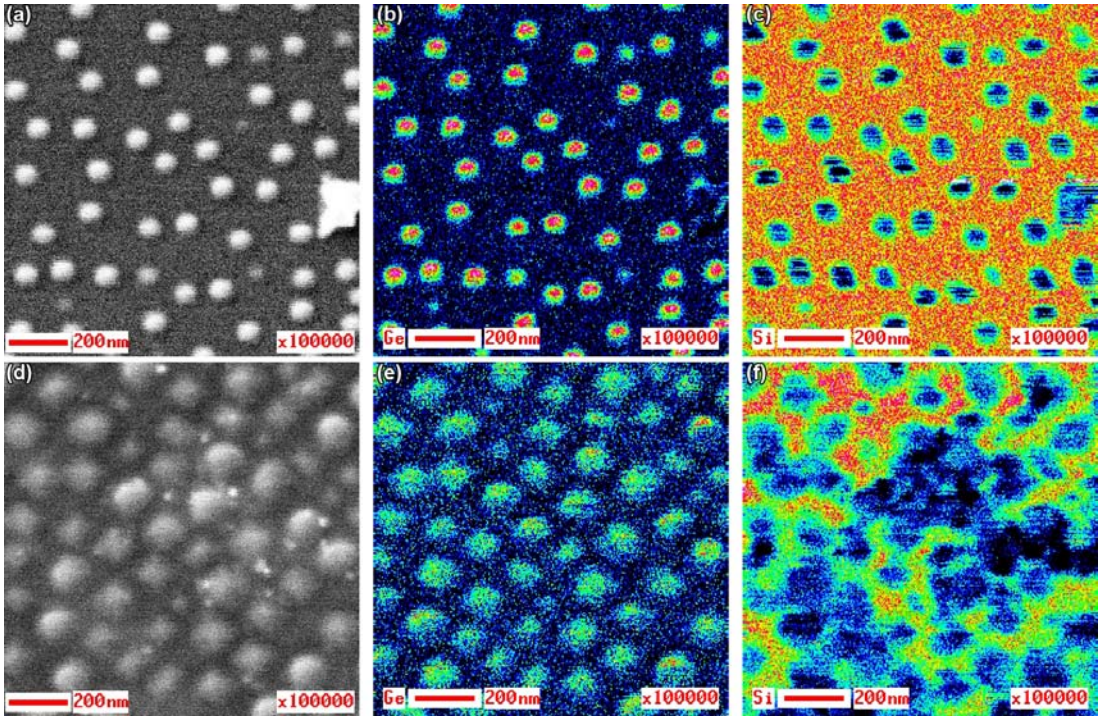

Fig. 4. Secondary electron images of the surface sections of A1 (a) and A2 (d) samples and corresponding to them Auger maps of Ge and Si in A1 (b, c) and A2 (e, f) samples, respectively.

The developed procedure was used to study the nature of the lateral elemental composition distribution on the sample surface containing GeSi/Si nanoislands and for understanding the relationship between this distribution and morphological features of the studied nanostructures.

The secondary electron image of A1 sample surface containing GeSi/Si nanoislands is shown in Fig. 4a. Auger maps of Ge and Si distribution registered from the same area of A1 sample are shown in Figs. 4b and 4c, respectively. The similar image (d) and corresponding to it Auger maps of Ge (e) and Si (f) were obtained for A2 sample. All of the above-mentioned pictures were registered at magnification 100 000.

4. Discussion

The analysis of secondary electron image of A1 sample shows the presence of two known types of GeSi/Si nanoislands on its surface. One of them has pyramidal faceting (p-clusters) and the other – dome-like faceting (d-clusters) [23, 24]. It is easy to see that dome-like faceting type in Fig. 4a prevails over the pyramidal faceting one, and lateral sizes of all formed nanoislands lay within the range from 40 up to 80 nm. The contours of the structures that appeared in the Auger maps of A1 sample (b, c) have the sharp boundaries and correspond to contours of GeSi/Si nanoislands presented in Fig. 4a. The maximum content of Ge corresponds to the central part of the nanoislands, and decrease of its concentration is observed on their periphery, which follows from Fig. 4b. It should be noted that the level of Ge content in the central part of the d-clusters on average is considerably higher than the level of its concentration in the central part of the p-clusters. The minimum concentration of Ge corresponds to the wetting layer. Lateral distribution of Si (c) is complementary to Ge distribution (b): sections enriched with germanium correspond to those with silicon depletion and *vice versa*. Thus, the maximum Si content corresponds to the wetting layer, and the minimum – to the central part of the nanoislands. The nanostructures of the d-type contain less silicon than the p-type structures.

It is easy to see on the surface section of A 2 sample shown in Fig. 4d that pyramidal faceting of the nanoislands prevails over dome-like faceting. The lateral sizes of all nanoislands vary within the range from 80 up to 150 nm. As in the case of A1 sample, the central parts of both nanoclusters types are enriched with Ge and the nanoislands of d-type have a higher concentration of Ge than the nanoislands of p-type. Also, from Fig. 4e it follows that the minimum Ge concentration at the surface of A2 sample corresponds to the wetting layer. The character of Si lateral distribution (Fig. 4f) is complementary to Ge Auger map of A2 sample. The minimum silicon content falls on the central parts of the

d-type clusters. The p-type clusters contain more silicon, whereas the maximum concentration of Si corresponds to the wetting layer. It should be noted that the surface of A2 sample contains carbon as a contaminant. The presence of the thin carbon film on the studied surface critically influences on the intensity of the low-energy Si_{LVV} Auger peak. This fact explains inhomogeneity of Si distribution on the wetting layer surface of A2 sample on the registered Auger map.

Analyzing the data shown in Fig. 4(a-f), it is easy to make the conclusion that dome-like and pyramidal nanoislands have Ge core surrounded with Si shell on both samples [25, 26]. The Ge content in the core of d-type clusters is always considerably higher than its content in the core of p-type clusters of the studied samples.

The formation of the cluster Si shell can be easily explained by the intensive interdiffusion development of Ge into the substrate and Si into the nanoisland on its surface [27, 28]. The bulk diffusion of Ge is slower than its surface one. Thus, the enrichment of the cluster core and the depletion of its shell by Ge occur. It is known that d-clusters due to the greater height are less stressed than p-clusters. The greater distances to the substrate and the lower gradients of stresses lead to a higher Ge content in the core of the domes.

Analyzing the lateral distribution of Si on the surface of A1 sample, it is easy to draw the conclusion that the interdiffusion process takes place the most intensively in the wetting layer. The wetting layer consists of pure Ge at the early stages of the planar film growth. The minimum concentration of Ge (Fig. 4b) and the maximum concentration of Si (Fig. 4c) are contained on the surface of the wetting layer after nucleation and in the process of the consequent nanoislands growth.

Some differences of the structural and morphological characteristics of the nanoislands in A1 and A2 samples should be noted. The presence of $Si_{0.9}Ge_{0.1}$ buffer layer in A2 sample has led to the increase of surface density and lateral sizes of the clusters. It is easily seen from Fig. 4d that pyramidal faceting of the clusters prevails over the dome-like faceting and the dispersion of nanoislands sizes is insignificant. This fact indicates that clusters were nucleated massively within a single generation in A2 sample. The nucleation process of nanoislands in A1 sample progressed slowly within several generations forming clusters of different facets and sizes in contrast to the previous case.

5. Conclusions

The use of AES and high-resolution SEM in combination with the developed procedure of the thermal drift correction is an effective instrument for analyzing the lateral elemental composition distribution on GeSi/Si nanoislands surface. The proposed method allows analyzing the clusters with the size of the structural elements down to 8…10 nm.

Overcoming the problem of thermal drift plays a key role in determining the lateral chemical composition distribution of GeSi/Si nanoclusters during operation at large magnifications in high spatial resolution mode. The long duration of the Auger maps registration procedure and weak removal of the heat released in the sample under the electron probe due to the low thermal conductivity of the sample are the factors contributing to the appearance of the thermal drift.

It was found that both the pyramidal and dome-like nanoclusters have the germanium core and the silicon enriched shell on the studied samples. Cores of dome-like nanoislands contain more Ge than cores of pyramidal nanoislands for all the samples. Such elemental composition distribution indicates an important role of surface interdiffusion of Ge into the substrate and Si into the cluster in the process of its nucleation and growth. The high concentration of Ge in the d-cluster core is a result of its greater sizes compared to the p-cluster. Germanium containing in the d-cluster core should overcome the greater diffusion path to the Si substrate. The Ge core of dome is closer to the equilibrium state as compared with the pyramid core due to the lower level of stresses in the d-cluster.

The presence of the $Si_{0.9}Ge_{0.1}$ buffer layer led to the increase of the lateral sizes and the surface density of the nanoclusters. In this case the nucleation of the nanoislands occurs massively and rapidly. The small size dispersion indicates this fact. The nucleation process, apparently, passes slowly and over several generations, forming the nanoislands with different faceting and sizes in absence of the buffer layer.

References

1. D. Bimberg, N. Ledentsov, Quantum dots: Lasers and Amplifiers // *J. Phys.: Condens. Matter*, **15**, p. R1063-R1076 (2003).
2. G. Masini, L. Colace, G. Assanto, Si based optoelectronics for communications // *Mater. Sci. and Eng. B,* **89**, p. 2-9 (2002).
3. E. Knill, R. Laflamme, G.J. Milburn, A scheme for efficient quantum computation with linear optics // *Nature,* **409**, p. 46-52 (2001).
4. Z. Yuan, B.E. Kardynal, R.M. Stevenson, A.J. Shields, C.J. Lobo, K. Cooper, N.S. Beattie, D.A. Ritchie, M. Pepper, Electrically driven single-photon source // *Science*, **295**, p. 102-105 (2002).
5. F. Ratto, G. Costantini, A. Rastelli, O.G. Schmidt, K. Kern, F. Rosei, Alloying of self-organized semiconductor 3D islands // *J. Experim. Nanosci.* **1**, p. 279-305 (2006).
6. J. Zhang, M. Brehm, M. Grydlikac, O.G. Schmidt, Evolution of epitaxial semiconductor nanodots and nanowires from supersaturated wetting layers // *Chem. Soc. Rev.* **44**, p. 26-39 (2015).
7. J.-N. Aqua, I. Berbezier, L. Favre, T. Frisch, A. Ronda, Growth and self-organization of SiGe nanostructures // *Phys. Repts.* **522**, p. 59-189 (2013).

8. G. Biasiol, S. Heun, Compositional mapping of semiconductor quantum dots and rings // *Physics Reports* **500**, p. 117-173 (2011).
9. Z.F. Krasil'nik, P.M. Lytvyn, D.N. Lobanov, N. Mestres, A.V. Novikov, J. Pascual, M.Ya. Valakh, V.A. Yukhymchuk, Microscopic and optical investigation of Ge nanoislands on silicon substrates // *Nanotechnology,* **13**, p. 81-85 (2002).
10. M.Ya. Valakh, V.O. Yukhymchuk, V.M. Dzhagan, O.S. Lytvyn, A.G. Milekhin, A.I. Nikiforov, O.P. Pchelyakov, F. Alsina, J. Pascual, Raman study of self-assembled SiGe nanoislands grown at low temperatures // *Nanotechnology,* **16**, p. 1464-1468 (2005).
11. M.Ya. Valakh, P.M. Lytvyn, A.S. Nikolenko, V.V. Strelchuk, Z.F. Krasilnik, D.N. Lobanov, A.V. Novikov, Gigantic uphill diffusion during self-assembled growth of Ge quantum dots // *Appl. Phys. Lett.* **96**, 141909 (2010).
12. J. Stangl, A. Daniel, V. Holý, T. Roch, G. Bauer, I. Kegel, T.H. Metzger, Th. Wiebach, O.G. Schmidt, K. Eberl, Strain and composition distribution in uncapped SiGe islands from X-ray diffraction // *Appl. Phys. Lett.* **79**, p. 1474-1476 (2001).
13. M. Valvo, C. Bongiorno, F. Giannazzo, A. Terrasi, Localized Si enrichment in coherent self-assembled Ge islands grown by molecular beam epitaxy on (001)Si single crystal // *J. Appl. Phys.* **113**, 033513 (2013).
14. U. Denker, M. Stoffel, O.G. Schmidt, Probing the lateral composition profile of self-assembled islands // *Phys. Rev. Lett.* **90**, 196102 (2003).
15. M.I. Alonso, M. Calle, J.O. Ossó, M. Garriga, A.R. Goñi, Strain and composition profiles of self-assembled Ge/Si (001) islands // *J. Appl. Phys.* **98**, 033530 (2005).
16. G. Katsaros, G. Costantini, M. Stoffel, R. Esteban, A.M. Bittner, A. Rastelli, U. Denker, O.G. Schmidt, K. Kern, Kinetic origin of island intermixing during the growth of Ge on Si (001) // *Phys. Rev. B* **72**, 195320 (2005).
17. O.G. Schmidt, U. Denker, S. Christiansen, F. Ernst, Composition of self-assembled Ge/Si islands in single and multiple layers // *Appl. Phys. Lett.* **81**, p. 2614-2616 (2002).
18. S.S. Ponomaryov, V.O. Yukhymchuk, P.M. Lytvyn, M.Ya. Valakh, Direct determination of 3D distribution of elemental composition in single semiconductor nanoislands by scanning Auger microscopy // *Nanoscale Res. Lett.* **11**, p. 103 (2016).
19. D. Briggs, M.P. Seah, *Practical Surface Analysis: Auger and X-ray Photoelectron Spectroscopy*, **1**. Chichester, John Wiley & Sons Inc., 1990.
20. G.A. Maximov, Z.F. Krasil'nik, A.V. Novikov, V.G. Shengurov, D.O. Filatov, D.E. Nikolitchev, V.F. Dryakhlushin, K.P. Gaikovich, Composition Analysis of Single GeSi/Si Nanoclusters by Scanning Auger Microscopy, Ch. 3, in: *Nanophysics, Nanoclusters and Nanodevices*, Ed. K.S. Gehar, p. 87-123. New York, Nova Science Publishers, 2006.
21. P. Frigeri, L. Seravalli, G. Trevisi, S. Franchi, Molecular Beam Epitaxy: An Overview, in: *Comprehensive Semiconductor Science and Technology*, Eds. P. Bhattacharya, R. Fornari, H. Kamimura, p. 480-522. Amsterdam, Elsevier, 2011.
22. M. Brehm, F. Montalenti, M. Grydlik, G. Vastola, H. Lichtenberger, N Hrauda, M.J. Beck, T. Fromherz, F. Schäffler, L. Miglio, G. Bauer, Key role of the wetting layer in revealing the hidden path of Ge/Si(001) Stranski–Krastanow growth onset // *Phys. Rev. B*, **80**, pp. 205321 (2009).
23. G. Medeiros-Ribeiro, A.M. Bratkovski, T.I. Kamins, D.A.A. Ohlberg, R.S. Williams, Shape transition of germanium nanocrystals on a silicon (001) surface from pyramids to domes // *Science*, **279**, p. 353-355 (1998).
24. A. Rastelli, M. Stoffel, G. Katsaros, J. Tersoff, U. Denker, T. Merdzhanova, G.S. Kar, G. Costantini, K. Kern, H. Kanel, O.G. Schmidt, Reading the footprints of strained islands // *Microelectron. J.* **37**, p. 1471-1476 (2006).
25. M.S. Leite, A. Malachias, S.W. Kycia, T.I. Kamins, R.S. Williams, G. Medeiros-Ribeiro, Evolution of thermodynamic potentials in closed and open nanocrystalline systems: Ge-Si:Si(001) islands // *Phys. Rev. Lett.* **100**, 226101 (2008).
26. G. Medeiros-Ribeiro, R.S. Williams, Thermodynamics of coherently-strained Ge_xSi_{1-x} nanocrystals on Si(001): Alloy composition and island formation // *Nano Lett.* **7**, p. 223-226 (2007).
27. R. Magalhaes-Paniago, G. Medeiros-Ribeiro, A. Malachias, S. Kycia, T.I. Kamins, R.S. Williams, Direct evaluation of composition profile, strain relaxation, and elastic energy of Ge:Si(001) self-assembled islands by anomalous x-ray scattering // *Phys. Rev. B*, **66**, 245312 (2002).
28. T.I. Kamins, G. Medeiros-Ribeiro, D.A.A. Ohlberg, R.S. Williams, Evolution of Ge islands on Si(001) during annealing // *J. Appl. Phys.* **85**, p. 1159-1171 (1999).